

## REPORT

# Integrating Plant Immune Models with Infection Cycles of *Cercospora coffeicola* in Uganda: Evaluating the Impact of Temperature, Rain, Wind and 3D Plant Architecture on Pathogen Dynamics

Group: Plant-pathogen modeling

Célia Lecat, Victor Robert Lambrecht, Mouad Leachouri and Marilyne HU

### Abstract

Brown eye spot, caused by the fungus *CERCOSPORA COFFEICOLA*, is a major challenge for coffee growers around the globe. In Uganda, where around five million people depend on coffee farming for their livelihood, this disease can reduce coffee yields by up to 50%, highlighting the need for effective disease management strategies.

To tackle this issue, we developed a model that simulates the infection cycle of *CERCOSPORA COFFEICOLA*. This model incorporates various climate factors such as temperature, wind, and rain to understand their impact on the disease's spread. Using climate data from NASA's POWER API, our model provides a realistic view of how these elements affect the disease's dissemination.

Our approach examines both the pathogen's life cycle, the coffee plants immune system, and the 3D plant architecture as well as the interactions between them. This method aims to identify the environmental conditions that favor disease progression and suggest potential intervention strategies. While our model currently offers a foundation for assessing infection rates and control measures, further validation and refinement are necessary for practical application.

**Keywords:** Mathematical modeling, Plant pathogens, *Cercospora coffeicola*, Disease modeling, Climate data integration, Coffee agriculture, Epidemic modeling

## 1. Introduction

Brown eye spot, caused by the fungal pathogen *CERCOSPORA COFFEICOLA*, is a disease affecting coffee plants worldwide. The main countries affected are undoubtedly those that rely most on coffee cultivation, such as Uganda, one of the largest coffee producers worldwide. Currently, five million people depend on this crop. When the pathogen infects a crop, it causes a significant decrease in harvest results of around 50%. Understanding the dynamics of infection by *CERCOSPORA COFFEICOLA* is important for developing disease management strategies in coffee-growing regions (Bock 1970).

### 1.1 Disease biology

*CERCOSPORA COFFEICOLA*, responsible of the Brown Eye Spot disease, is a pathogenic fungus that significantly affects coffee cultivation. This disease, due to its characteristic symptoms, is recognized

as one of the most damaging to coffee plantations. It mainly targets the leaves and berries of the coffee tree, leading to a considerable decrease in production. (Rivillas, n.d.)

The presence of this disease can be visually detected due to its distinctive symptoms. On the leaves, the pathogen manifests as small round spots, ranging from chlorotic to slightly reddish-brown or necrotic, measuring between 1 and 3 mm in diameter. These lesions evolve to form a grayish center surrounded by a brown concentric crown. Over time, the lesions become black and dry, and yellow spots may appear nearby. Sometimes, the crown may develop irregularly and without precise delineation. (Rivillas, n.d.)

On the berries, whether they are green or ripe, the lesions begin as small, isolated, reddish points. As the fruit matures, these points enlarge and penetrate deeper, especially if the fruit is protected from the sun. Green fruits affected by the disease undergo premature ripening and fall prematurely from the tree. Berries affected by the disease may be partially or completely covered, showing signs of drying and darkening. (Rivillas, n.d.)

The life cycle of *CERCOSPORA COFFEICOLA* is a crucial aspect to consider when modeling the dynamics of this pathogen. The phases of this cycle can be classified in ascending order as follows: (Frédéric Boyer 2019)

- **Spore deposition** : Spores of *CERCOSPORA COFFEICOLA* are deposited on coffee leaves, branches, or berries, often carried by wind or water splashes from rain. These spores can also be present in surrounding plant debris. (Imbusch et al. 2020)
- **Spore germination** : When conditions are favorable, including sufficient humidity and adequate temperature, spores of *CERCOSPORA COFFEICOLA* germinate on the surface of leaves or berries, forming germ structures called hyphae. (Silva et al. 2015)
- **Spore incubation and lesion formation** : The fungus's hyphae then penetrate the tissues of the host plant, colonizing cells and growing inside. During this phase, which can take from a few days to weeks depending on environmental conditions, no visible lesions are yet present. (Ni, Lin, and Wu 2020)
- **Mature lesions** : After an incubation period, characteristic lesions begin to appear on infected leaves or berries. These lesions appear as round or irregular spots, ranging in color from brownish to black, often surrounded by a discolored area. They may continue to spread and grow as long as conditions are conducive to fungal growth. (Rivillas, n.d.)
- **Lesion death** : Over time, mature lesions of *CERCOSPORA COFFEICOLA* may dry out, blacken, and ultimately die.

The life cycle described for *CERCOSPORA COFFEICOLA* is inferred based on that of *CERCOSPORA BETICOLA* affecting beets, as these two share significant epidemiological similarities. Additionally, the cycle may repeat multiple times during the coffee growing season.

## 1.2 Plant immune system model

Plants are constantly exposed to potential pathogens and pests. To survive, they have developed a variety of passive and active defense mechanisms that can be broadly categorized into structural defenses, preformed chemical defenses or constitutive immunity, induced chemical defenses, molecular recognition systems, signal transduction pathways (Doughari et al. 2015), systemic acquired resistance

(SAR), RNA silencing mechanisms (Muhammad et al. 2019), and interactions with the microbiome (Ali, Tyagi, and Bae 2023).

The first line of defense in plants consists of physical barriers. The cell walls, composed of cellulose, hemicellulose, and lignin, form a tough barrier against pathogen entry. Additionally, the cuticle, a waxy layer covering the epidermis of leaves and stems, prevents pathogen invasion. Stomatal closure is another mechanism, where stomata can close to block pathogens from entering through these pores (Doughari et al. 2015).

Plants produce various antimicrobial and antifungal compounds as a preemptive defense mechanism. Phytoanticipins, such as saponins and glucosinolates, are constitutively present in the plant. Secondary metabolites, including alkaloids, flavonoids, and terpenoids, also possess antimicrobial properties that help in defending against pathogens (see Kant et al. 2015 and Osbourn 1996). Notably, coffee plants are cultivated primarily for their production of the alkaloid caffeine, a molecule that originally functions as a component of the plant's immune system (Sledz et al. 2015).

In response to pathogen attack, plants can synthesize new defensive chemicals. Phytoalexins are antimicrobial compounds produced specifically in response to pathogen infection. Reactive oxygen species (ROS), such as hydrogen peroxide, are also generated and can damage invading pathogens (Doughari et al. 2015).

Plants detect pathogen-associated molecular patterns (PAMPs) through specific receptors. Pattern recognition receptors (PRRs) recognize PAMPs, such as bacterial flagellin or fungal chitin, triggering immune responses. In addition, effector-triggered immunity (ETI) occurs when plants recognize specific pathogen effector proteins via resistance (R) proteins, leading to a stronger immune response (Bentham et al. 2020).

Upon pathogen detection, various signaling pathways are activated. The salicylic acid (SA) pathway is typically involved in defense against biotrophic pathogens. The jasmonic acid (JA) and ethylene (ET) pathways are often associated with defense against necrotrophic pathogens and insect herbivores (see Ding et al. 2022).

Plants lack an adaptive immune system, but Systemic Acquired Resistance (SAR) provides long-lasting protection against a broad spectrum of pathogens and can be seen as a form of plant memory. Priming is a process where previous exposure to a pathogen can enhance the plant's response to subsequent attacks. Signaling molecules, such as methyl salicylate, can travel throughout the plant to induce resistance in distant tissues (Conrath 2006).

Plants also use RNA interference (RNAi) to degrade viral RNA. Small interfering RNAs (siRNAs) target and degrade viral RNA, preventing virus replication (Muhammad et al. 2019). Microbes also play a role in enhancing plant immunity. Endophytes and rhizosphere microbes can outcompete pathogens or induce plant immune responses (Ali, Tyagi, and Bae 2023).

### **1.3 Aims and objectives**

To address this need, we propose a modeling approach to simulate the infection cycle of *CERCOSPORA COFFEICOLA* in Uganda. By developing this comprehensive model, we aim to elucidate interplays between climate factors such as temperature, wind, and rain, and their influence on the epidemiology of coffee leaf spot. Then, we develop a computer simulation that yields more concrete results.

Historically, the study of *Cercospora* infections has predominantly focused on the plant-pathogen interaction, with substantial progress made in elucidating the plant's defensive mechanisms. However, a comprehensive understanding of the pathogen's life-cycle, transmission dynamics, and infection mechanisms remains underdeveloped. Integrating a detailed pathogen-specific model into existing plant models is essential to capture the full complexity of *Cercospora*-related diseases. This work will then be integrated with a plant growth model using the *MIMIC* platform developed by the French agricultural research organization *CIRAD* (Triki et al. 2023). This platform facilitates the coupling of models to simulate plant-environment interactions.

We aim to develop a robust, **pathogen-centric** model of *Cercospora* infections. This model will be designed to integrate seamlessly with the existing plant model on the *MIMIC* platform [*not implemented yet, the coupling is done locally in our code for now*], facilitating a holistic simulation of the *Cercospora* infection process. By focusing on the pathogen, we seek to uncover critical aspects of its biology, including spore dispersal, infection initiation, and progression within host tissues.

## 2. Methods

In this section, we lay out the foundational hypotheses for our study. We then derive a plant model that encapsulates the trees' spatial distribution and immune responses, and a pathogen model based on the life-cycle presented in the introduction.

### 2.1 Hypotheses

This section is supposed to be read in parallel with the next sections as it provides contextual justifications of our modelling approaches. Some of the hypotheses present clear limitations, that could be discussed in a further section.

- **Hypothesis 1:** We consider that temperature conditions do not hinder spore germination, i.e., temperature doesn't stop a spore from germinating. It only slows a lesion's growth rate.
- **Hypothesis 2:** In our model, we assume that spore production comes to a complete halt after the spore dries out, i.e., dies.
- **Hypothesis 3:** We assume that the durations of deposition, germination and maturity are fixed and do not depend on climate variables (see Fig. ??).
- **Hypothesis 4:** As the effect of *splashing* is roughly local, we assume that the rain droplets only carry spores from one leaf to another within the same coffee tree.
- **Hypothesis 5:** We consider that the wind doesn't affect the direction in which the spore spread is happening. The spread is thus considered isotropic.
- **Hypothesis 6:** Each coffee plant has a different number of leaves, all assumed to have a uniform area denoted by  $\Gamma \in \mathbb{R}_+$ . This simplification aids in standardizing calculations for pathogen spread.
- **Hypothesis 7:** Only fully grown lesions are attacked by the plant's offensive immunity system.
- **Hypothesis 8:** The systemic immune response, and SAR is an on and off switch that does not depend on the intensity of the infection

### 2.2 Spatial distribution of the hosts

A *field* of coffee trees is modeled as an  $\mathbb{R}^2$  plane. A *plant*, specifically a coffee tree can reside in any coordinates  $(x, y) \in \mathbb{R}^2$ . We will use the L-System to model the Tree architecture, which is extensively described here (Prusinkiewicz et al. 1996). We will provide a short overview of the system:

### 2.2.1 L-System Mathematical Formalism

An L-system (Lindenmayer system) is a parallel rewriting system and a type of formal grammar. It is defined by:

- **Alphabet:** A set of symbols that can be used to create strings.
- **Axiom:** A string of symbols from the alphabet that serves as the initial state.
- **Production Rules:** A set of rules that expand each symbol into a larger string of symbols.

### 2.2.2 Formal Definition

An L-system is a tuple  $G = (V, \omega, P)$  where:

- $V$  (Alphabet): A finite set of symbols.
- $\omega$  (Axiom): A non-empty string of symbols from  $V$  that is the initial string.
- $P$  (Production Rules): A finite set of production rules that define how symbols can be replaced with other symbols. Each rule has the form  $A \rightarrow \phi$ , where  $A$  is a symbol from  $V$  and  $\phi$  is a string of symbols from  $V$ .

### 2.2.3 Generating Trees

L-systems are effective in generating tree-like structures due to their ability to create complex patterns from simple iterative rules. This is achieved through:

- **Branching Mechanism:** L-systems often include symbols for branching (e.g., "[" and "]" in extended L-systems). These symbols allow for the representation of branches by indicating a return to a previous state in the string.
- **Angle Control:** Symbols like "+" and "-" are used to control the angle of growth, allowing the formation of natural, fractal-like structures.
- **Recursive Growth:** The iterative application of production rules enables the creation of self-similar structures, a characteristic feature of many natural forms such as trees.

### 2.2.4 Our Trees:

Here is a parameter table that will be used to generate our 3D trees:

**Table 1.** L-System Parameters and Descriptions

Parameter	Value	Description
Position	N/A	The specific point or index in the sequence or structure being generated.
Axiom	F	The initial string from which the L-system starts.
Iterations	3	The number of times the production rules are applied to the axiom. More creates more realistic trees but is computationally very expensive.
Initial Length	1 unit	The starting length of each segment before any scaling is applied.
Angle	25.7 degrees	The angle by which the direction changes when encountering specific symbols (e.g., "+" and "-").
Length Decrease Factor	0.7	The factor by which the length of segments decreases with each iteration. Allows for progressive smaller branches.

### 2.3 Plant immune system model

Modeling different interactive components of the plant immune system can be complex, given that they operate on different spatial and temporal scales and require distinct modeling approaches, including ordinary differential equations (ODEs), graph networks, and population dynamics. Within this remarkable heterogeneity of the plant's immune system, it is also recognized that plants exhibit a broad general immune response and susceptibility, which will be the focus of our modeling efforts.

For clarity and simplification, we categorize the immune response into two parts:

#### 2.3.1 Local Immunity

Local immunity encompasses several mechanisms. Cell wall reinforcement reduces germination from spore deposition, necrosis limits the extent of pathogen infection before the leaf falls off, and the production of defensive compounds slows down pathogen progression.

#### 2.3.2 Systemic Immunity

Systemic immunity involves the priming of defense mechanisms. Signaling molecules such as salicylic acid (SA), jasmonic acid (JA), and ethylene (ET) travel through the plant, preparing it for defense. Long-lasting protection, facilitated by Systemic Acquired Resistance (SAR), results in increased structural defenses and the production of defensive compounds. Each plant has a systemic immunity factor ( $I$ ) that it shares among its branches. This factor changes when a branch is attacked, increasing logarithmically to a maximum value ( $MAX_{SAR}$ ) and decreasing over time, also logarithmically. The increase is not immediate, typically taking a couple of weeks to reach its maximum value.

Additionally, plant immune responses can be classified into constitutive immunity and induced immunity. For modeling purposes, we assume that leaves on the same branch share the same immunity.

### 2.4 Immune Protection Layers

We identify three layers of immune protection:

#### 2.4.1 Protection Against Pathogen Entry

Each branch has a structural immunity value ( $S_{struct}$ ), which reduces the growth of the pathogen inside the host. This value ranges from 1 (no immunity) to 0 (maximal immunity) and is the sum of baseline immunity ( $S_{base}$ ), shared across all branches of the same tree, and a branch-specific factor ( $S_{ind}$ ), which starts at 1 and decreases upon an induced immune response, with a minimum value of 0.

#### 2.4.2 Necrosis Immunity

Necrosis immunity ( $N_{imm}$ ) determines the maximum pathogen-affected area for each leaf. It ranges from 0 (immediate necrosis) to 1 (no necrosis). This constitutive immunity parameter is shared by all branches and leaves of the same tree and does not change over time.

#### 2.4.3 Offensive Immunity

Offensive immunity ( $O_{imm}$ ) reduces pathogen spread within the plant via the production of chemical compounds. It is the sum of the plant's baseline immune reactivity ( $I$ ) and a branch-specific immunity factor ( $O_{ind}$ ), which increases from 0 to a maximum induced value ( $MAX_{ind}$ ) when the plant is attacked.

**Table 2.** Description of variables related to plant immunity.

Variable	Domain	Description
$S_{struct}$	$[0, 1]$	Structural immunity of each branch.
$S_{base}$	$[0, 1]$	Baseline structural immunity, shared across all branches.
$S_{ind}$	$[0, 1]$	Induced structural immunity of a specific branch, decreasing from 1 to 0.
$N_{imm}$	$[0, 1]$	Necrosis immunity, shared across all branches.
$O_{imm}$	$[0, MAX_{ind} + MAX_{SAR}]$	Offensive immunity of each branch.
$O_{ind}$	$[0, MAX_{ind}]$	Offensive immunity specific to the branch, that is induced by the presence of pathogens.
$I$	$[0, MAX_{SAR}]$	Systemic immunity, shared across all branches. It increases if the plant is attacked and represents a global state of immune readiness.
$P$	-	The number of pathogens on a given leaf. This number will be used to decide when the plant triggers an immune reaction.
$R$	$[0, 1]$	The speed of increase and decrease of the SAR.
$MAX_{SAR}$	$[0, \frac{1}{2}]$	Maximal value the systemic immunity can take.
$MAX_{ind}$	$[0, \frac{1}{2}]$	Behaves in the same way as $MAX_{SAR}$ , for the same reasons. Note that their sum cannot exceed 1.

## 2.5 ODE Model for Immune Variables

To model the immune responses, we define the following variables and their respective spaces:

The tree  $T$  is defined by its position, number of branches, and specific immune parameters. Let  $B_i$  be a list of branches indexed by  $i$ , a natural number between 0 and  $N$ , where  $N$  is the total number of branches.

### 2.5.1 Derivatives and ODEs

The equations governing the variables are defined as follows: **Local immunity:**

#### 2.5.2 Structural Immunity

$$\begin{cases} S_{struct} = S_{ind} + S_{base} \\ \frac{dS_{base}}{dt} = 0 \\ \frac{dS_{ind}}{dt} = S_{ind} \cdot (\mathbf{1}_{\{P>10\}} - S_{ind}) \end{cases} \quad (1)$$

With  $P$  being the number of pathogens on the branch. 10 is being set as the threshold for inducing the infection.

#### 2.5.3 Necrosis Immunity

$$\begin{cases} \frac{dN_{imm}}{dt} = 0 \end{cases} \quad (2)$$

Necrosis immunity ( $N_{imm}$ ) is constant over time.

#### 2.5.4 Offensive Immunity

$$\begin{cases} O_{imm} = O_{ind} + I \\ \frac{dO_{ind}}{dt} = O_{ind} \cdot (\mathbf{1}_{\{P>10\}} - \frac{O_{ind}}{MAX_{ind}}) \end{cases} \quad (3)$$

With  $I$  following these equations : **Systemic immunity:**

### 2.5.5 Systemic Immunity

$$\left\{ \frac{dI}{dt} = R \cdot I \cdot (\mathbf{1}_{\{P>10\}} - I) \right. \quad (4)$$

where  $R$  is the rate of increase and decrease of the SAR. It is very low  $< \frac{1}{10}$  to model slow immune adaptation throughout the entire plant. Note that  $P$  here describes the pathogen content of **any** branch, meaning that only one infected branch is sufficient to trigger a global immune response. Also, note that if multiple branches are infected, there is no change in the global intensity of the immune response. (see Hypothesis 8, Section 2.1)

### 2.5.6 Model Structure

The model considers a tree  $T$ , characterized by its position, number of branches, and specific immune parameters. The tree is defined as  $T = (N, (x, y), S_{\text{base}}, N_{\text{imm}}, I)$ . Each branch  $B_i$  inherits tree-level variables and has branch-specific variables  $B_i = (S_{\text{ind}}, O_{\text{ind}}, O_{\text{imm}}, S_{\text{struct}})$ :

- Tree-level variables:  $S_{\text{base}}, N_{\text{imm}}, I$
- Branch-level variables:  $S_{\text{struct}}, S_{\text{ind}}, O_{\text{imm}}, O_{\text{ind}}$

### 2.5.7 Interaction with growth model [not done yet]

Plants have to perform a trade-off between immune function and plant growth and berry production.

## 2.6 Pathogen model

The *CERCOSPORA COFFEICOLA* pathogen infects leaves through *spores* that germinate and develop into *lesions*. **We consider these spores, which eventually develop into lesions, as the individuals of our pathogen population.**

In our coding methodology, we utilize a **cohort-based approach** (inspired from Triki's work (Triki et al. 2023)). Rather than analyzing each lesion separately, we organize them based on their **deposition date and the leaf on which were deposited**, forming what we term a *pathogen cohort*. This approach acknowledges that in our model, individuals deposited on the same day and on the same leaf share the same fate.

To model the development of lesions over time and space, we construct a mechanistic sub-model for each stage of the pathogen's life cycle (see Fig.??).

### 2.6.1 Deposition

After being transported by wind or rain splashing (see Subsection 2.6.4), the spore is *deposited* on a leaf where it remains inactive, without germinating, for a fixed duration  $d \in \mathbb{R}_+$  (see Hypothesis 3, Section 2.1).

### 2.6.2 Germination

When the time  $d$  has elapsed, not every spore will *germinate*. Germination occurs with a probability factor  $P_g \in [0, 1]$ , which is directly proportional to the free area  $A \in \mathbb{R}_+$  on the plant (see Hypothesis 1, Section 2.1), representing the space not already occupied by other lesions.  $P_g$  is also proportional to a function  $f$  of relative humidity  $H$ , which takes values ranging from 66% to 100%:

$$f(H(t)) = \exp \left( -\frac{(H(t) - \mu)^2}{2\sigma^2} \right) \quad (5)$$

where  $\mu = 0.942$  and  $\sigma = 0.07$  is fitted with article's data (RAM and MALLAIAH 1996). Hence the probability  $P_g$  of germination can be written as:



$$P_g = \frac{A(t)}{N_{\text{imm}} \cdot \Gamma} \times f(H(t)) \quad (6)$$

where  $\Gamma$  is the leaf area (see Hypothesis 6, Section 2.1). The factor  $N_{\text{imm}}$  accounts for *necrosis*, which causes leaves to fall after an infection severity threshold is crossed. If  $N_{\text{imm}} = 3$ , then the leaf will commit necrosis when one third of its area has been infected, stopping further pathogen growth.

The area  $a \in \mathbb{R}_+$  occupied by a lesion depends on both the age of the lesion and the temperature  $\theta \in \mathbb{R}$ .

If the lesion is mature (see Subsection 2.6.3) or dead (see Subsection 2.6.5), it occupies a constant surface area  $a_{\text{max}} \in \mathbb{R}_+$ . However, if the lesion is in the germination state, it occupies a variable area that converges to the maximum value  $a_{\text{max}}$ :

$$a(t) = a_{\text{max}} \left( \frac{1}{1 + e^{-\alpha(t) \cdot t}} - \frac{1}{2} \right) \quad (7)$$

where  $\alpha \in \mathbb{R}_+^*$  is a coefficient determining the convergence speed of  $a$ . It depends on the temperature  $\theta$ , as well as the plant's structural immunity.

$$\alpha(t) = \frac{S_{\text{struct}}}{1 + |\theta(t) - \theta_{\text{opt}}|} \quad (8)$$

$\theta_{\text{opt}} \in \mathbb{R}_+$  being the optimal temperature for pathogen development. If  $S_{\text{struct}}$  is low the pathogen will grow slowly inside the host, and if large it can grow unencumbered.

Hence, the free area for a plant  $P$  is:

$$A = \Gamma - \sum_{\text{lesion} \in P} a_{\text{lesion}} \quad (9)$$

### 2.6.3 Maturity

After a fixed duration  $g \in \mathbb{R}_+$  (see Hypothesis 3, Section 2.1), a lesion transitions unconditionally to the *adult* stage, where **spore production** occurs. Each adult lesion continuously produces spores at a constant rate  $r \in \mathbb{R}$ .

### 2.6.4 Dispersal

CERCOSPORA COFFEICOLA spores are primarily dispersed by **wind**, with **rain** also facilitating dispersal through *splashing* (see Hypothesis 4, Section 2.1), propelling spores from one leaf to another.

Spore dispersal integrates spatial aspects into the model, including two scales (inspired by the work of F. van den Bosch and Zadoks 1999):

- *Within-plant dispersal*: Spores move between leaves within the same canopy.
- *Between-plant dispersal*: Spores travel between different plants.

#### Within-plant dispersal

Utilizing the plant model in ??, within-plant dispersal is modeled using a Gaussian probability density function. The probability density that a spore produced by a lesion on a leaf at altitude  $z_0 \in \mathbb{R}$  lands on a leaf at altitude  $z$  is given by:

$$f_{\text{wpd}}(z_0, z) = \frac{1}{\sqrt{2\pi}\sigma} e^{-\frac{(z-m)^2}{2\sigma^2}} \quad (10)$$

Note that we are only using the vertical direction,  $z$ . This is because, for a single tree, the primary variation in leaf distance is determined by the  $z$  component of the position.

Wind and rain influence dispersal. Thus, we assume that these climate variables control the standard deviation  $\sigma \in \mathbb{R}_+^*$  and mean  $m \in \mathbb{R}$ . Wind speed  $w \in \mathbb{R}_+$  determines spore dispersal range, hence  $\sigma = Kw$ , where  $K \in \mathbb{R}_+$  is a proportionality constant.

To account for splashing, which generally propels spores to upper leaves, a positive perturbation  $\varepsilon \cdot \rho$  is added to  $m$ , where  $\rho \in \mathbb{R}_+$  is rainfall depth and  $\varepsilon \in \mathbb{R}_+$  is a constant (see Fig. ??).

### Between-plant dispersal

Between-plant dispersal follows a similar Gaussian approach, with spores propagating from a source plant to receiving plants. This time the main The probability density function corresponding to dispersal from a coffee tree at  $\mathbf{p}_0 = (x_0, y_0)$  to a tree at  $\mathbf{p} = (x, y)$  is:

$$f_{bpd}(\mathbf{p}_0, \mathbf{p}) = \frac{1}{2\pi\sqrt{\det \Sigma}} \exp \left( -\frac{1}{2}(\mathbf{p} - \boldsymbol{\mu})^T \Sigma^{-1}(\mathbf{p} - \boldsymbol{\mu}) \right) \quad (11)$$

Here,  $\Sigma \in \mathbb{R}^{2 \times 2}$  denotes the covariance matrix indicating dispersal range, and  $\boldsymbol{\mu}$  represents the source position  $\mathbf{p}_0$ .  $\Sigma$  is a scalar matrix directly proportional to the wind speed  $w$  (see Hypotheses 4 and 5, Section 2.1).

#### 2.6.5 Death

There are two ways for pathogen cohorts to die:

After producing spores for a fixed duration  $a \in \mathbb{R}_+$  (see Hypothesis 3, Section 2.1), a lesion enters the *death* phase. In this stage, the lesion's activity reduces to occupying a region on the leaf's surface, inhibiting nearby spore germination (see Hypothesis 2, Section 2.1).

Adult populations of cohorts are also subject to the plant's offensive immune system (see Hypothesis 7, Section 2.1), and have a certain probability of dying each time step, given by the following equation. For a branch  $i$ , and a cohort  $c$ :

$$P_{\text{death}}(i, c) = O_{\text{imm}}(i) \quad (12)$$

## 2.7 Climate Data

The data was obtained from the National Aeronautics and Space Administration (NASA) Langley Research Center (LaRC) Prediction of Worldwide Energy Resource (POWER) (NASA 2024) Project funded through the NASA Earth Science/Applied Science Program.

This service provides reliable climate data, including daily temperature at a height of 2 meters above ground, humidity, rainfall, and wind speed at Kampala for the year 2018. These variables are crucial for understanding the environmental conditions that influence *CERCOSPORA COFFEICOLA*'s infection and spread.

The NASA POWER data is relevant due to its high temporal resolution and global coverage, making it an ideal source for agricultural and ecological studies. The reliability of NASA POWER data is supported by its use in various scientific research and operational applications, ensuring accurate climate information. (Kadhim Tayyeh and Mohammed 2023)

## 2.8 Field Data

The parameter calibration data were collected as part of the ROBUST project (EU 2020), on a plot located at the NACORI station in Uganda. Data collection occurred during two distinct periods: mid-February 2023 and late March 2023.

To validate intra-branch dynamics, a sample of 10 trees from 2 different clones was selected, resulting in a total of 20 trees distributed across 7 of the 15 blocks within the plot. Four branches per tree were monitored. For each fruit cluster, the total number of fruits, the number of fruits

exhibiting a spot due to (Red Blotch Disease) RBD, and the number of fruits showing multiple spots due to RBD were recorded.

A comprehensive examination of all branches on 30 trees was conducted, noting the presence or absence of RBD on each branch.

## 2.9 Table of parameters

**Table 3.** Parameters controlled in the study.

Parameter	Description	Units	Source
$\theta$	Temperature	$^{\circ}\text{C}$	NASA POWER API
$H$	Humidity	%	NASA POWER API
$\rho$	Rainfall	mm	NASA POWER API
$w$	Wind speed	m/s	NASA POWER API
$N$	Number of pathogen lesions	Count	Laboratory analysis
$\Delta z$	Difference of altitude between two leaves/branches.	m	Calibrated on ROBUST PROJECT
$\Gamma$	Area of a coffee leaf	$\text{m}^2$	Calibrated on ROBUST PROJECT
$a_{max}$	Maximum area of a lesion	$\text{m}^2$	Calibrated on ROBUST PROJECT
$d$	Deposition duration	days	Calibrated on ROBUST PROJECT
$g$	Germination/development duration	days	Calibrated on ROBUST PROJECT
$a$	Maturity duration	days	Calibrated on ROBUST PROJECT
$r$	Spore production rate	spores/day	Calibrated on ROBUST PROJECT
$\theta_{opt}$	Optimal temperature for disease development	$^{\circ}\text{C}$	Calibrated on ROBUST PROJECT
$S_{base}$	Baseline structural immunity	-	Calibrated on ROBUST PROJECT
$N_{imm}$	Necrosis immunity	-	Calibrated on ROBUST PROJECT
$MAX_{ind}$	Maximum induced offensive immunity	-	Calibrated on ROBUST PROJECT
$MAX_{SAR}$	Maximum systemic acquired resistance	-	Calibrated on ROBUST PROJECT
$R$	Rate of increase and decrease of SAR	$< 1/10$	Calibrated on ROBUST PROJECT

## 2.10 Empirical validation

[Not done yet]

## 3. Results and Discussion

### 3.1 Tree architecture

With  $N = 10$  trees, generated randomly with the parameters found in 1 .

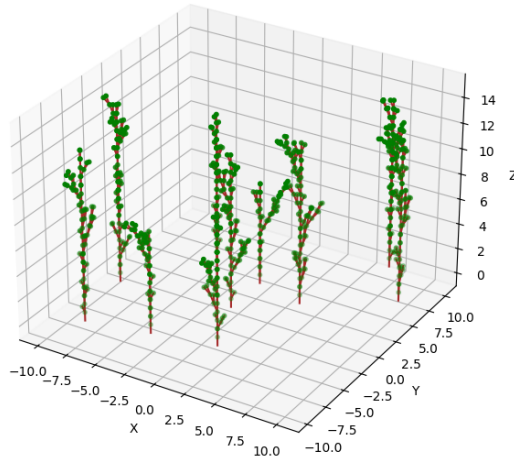


**Figure 1.** Example of a field generated with the L-System

In the following, we present the results of our simulation. We take a look at the number of lesions infecting coffee plants over time. The findings are then discussed in relation to previous studies.

To understand the results, we will first present our initial conditions: the distribution of trees across the field, the number of leaves on each tree, and the initial state of the pathogen individuals.

### 3.2 Initial conditions

As can be seen in Figure ??, the simulation starts with a minimalist field of five coffee trees. Three trees, at positions  $(1.2, 0)$ ,  $(2, 0)$  and  $(2, 1)$  are labeled “*healthy*”, that is, all their leaves are free of *CERCOSPORA COFFEICOLA* spores. On the other side, we add two trees at positions  $(0, 0)$  and  $(0, 1)$ . These two trees are labeled “*infected*”. In this context, this label is used abusively to refer to trees that are hosts to some *CERCOSPORA* spores.

The table 4 encapsulates all the starting conditions, with the number of leaves on each tree and the corresponding numbering of trees used in the plots in the next sections.

**Table 4.** State of the field at  $t = 0$

Plant ID	Position	Number of Leaves	Number of Starting Spores	State
1	(0,0)	10	A cohort of 20 spores	Infected
2	(0,1)	12	A cohort of 10 spores	Infected
3	(1.2,0)	14	0	Healthy
4	(2,0)	10	0	Healthy
5	(2,1)	20	0	Healthy

### 3.3 Total number of lesions

The total number of lesions in the coffee field, resulting from the simulation, is shown in Figure 2. Note that we only plot the number of lesions, and not that of spores that didn't develop into lesions yet.

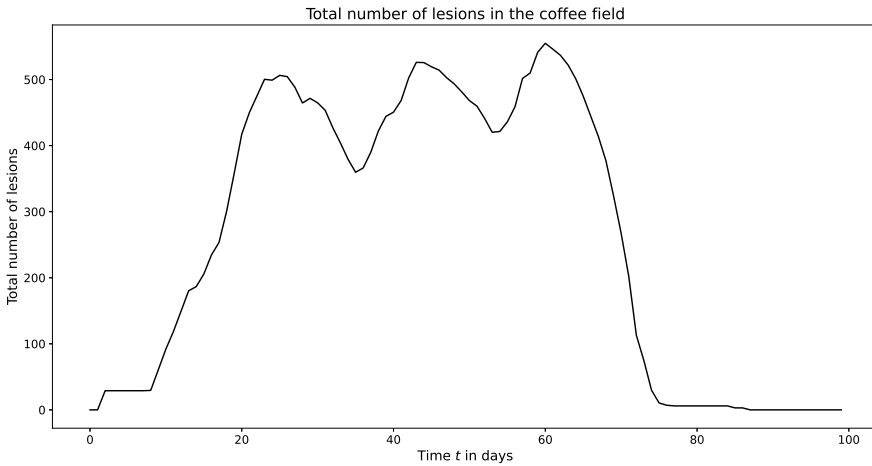


**Figure 2.** The total number of lesions in the coffee field as a function of time

We can see a clear “*population boom and bust*” or a “*population pulse*”, that is, the trend is characterized by a rapid increase in population followed by an other rapid decline back to zero. This could be interpreted by looking at limited resources available for the *CERCOSPORA COFFEICOLA* pathogen. The first increase in the total number of lesions across the coffee trees can be explained by the dispersal of the spores produced by the first fully developed lesions. The rapid decline at the end is due to the last lesions dying out without producing fertile spores, as all the coffee trees are virtually dead and no longer provide a suitable environment for spore germination.

One observation that stands out is the initial phase where the total number of lesions exhibits a slight plateau before experiencing a rapid increase. This plateau occurs because, initially, only spores are deposited on the leaves of the affected trees, and there are no fully grown lesions present. Therefore, the small increase in lesion count during this phase corresponds to these spores transitioning to the germination state. The subsequent plateau is a result of these germinating spores that haven't reached maturity yet. Once they became capable of producing additional spores that manifested as fully mature grown, the population bloomed again.

Within the initial two months, the population peaks at approximately 500 individuals. This sudden surge can be explained by the favorable environmental conditions and abundant food sources available during this period. Specifically, it appears that spores successfully reached the tree with the highest leaf count, that provided an ideal environment for their growth. Subsequently, aided by wind and splashing effects, the spores propagated from one leaf to another, contributing to the rapid population increase.

During the population peak phase, spanning from the end of month 1 to approximately the middle of month 3, fluctuations in the number of lesions are observed, characterized by three local peaks. To analyze this phase more thoroughly, the plotted results need further refinement. Therefore, in the next section, we delve into studying the number of lesions on individual coffee trees.

### 3.4 Number of lesions on each plant

In Figure 3, one can see a population pulse of the pathogen on each coffee tree separately, each rapid decline to 0 indicating the death of a plant. Naturally, the previous graph is just the superposition of the five individual graphs on the next figure.

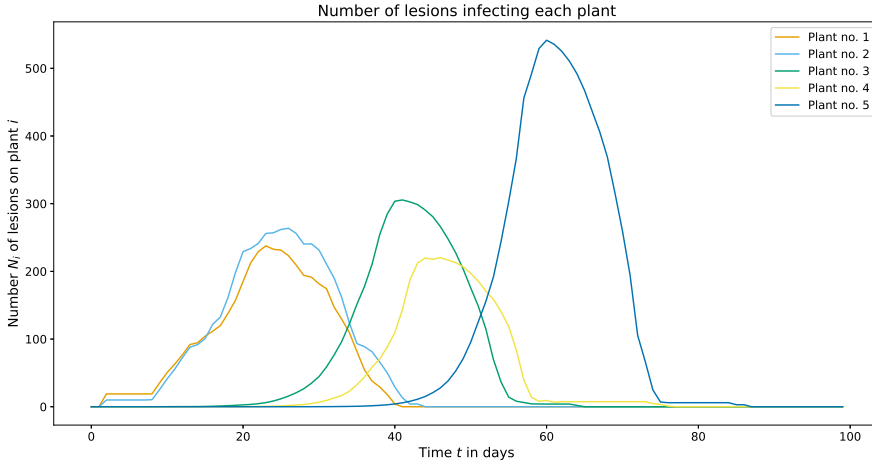


**Figure 3.** The number of lesions on each coffee tree as a function of time

Upon initial observation, it becomes apparent that plants with identifiers 1 and 2, which were initially infected, are the first to experience a surge in pathogen population. They reach their peak population levels at roughly the same time, given their similar leaf counts. However, upon closer examination, a slight delay is observed, as the second plant has marginally more leaves compared to the first one.

Another contributing factor to the delay is the spatial arrangement of the coffee trees. The initial infection spreads first to tree no. 3, which is the closest to the initially infected trees. This proximity results in a propagation delay of roughly 20 days between the peaks of trees 1 and 3. Conversely, the tree no. 5 becomes infected last (with a delay of roughly 40 days), being the farthest from the initial source of infection.

An additional realistic aspect of our model is that the population on each individual tree reaches a different peak value. This peak value reflects the amount of resources a tree provides for the pathogen. For instance, tree no. 5 naturally hosts the highest population bloom as it has the most leaves. Conversely, trees no. 1 and 4 host the lowest population peak values as they have each around 10 leaves.

## 4. Conclusion

In this study, we developed a mathematical model to simulate the infection dynamics of *CERCOSPORA COFFEICOLA* in coffee plants, intended for application in Uganda for data collected as part of a European project (ROBUSTE). The model brings together plant growth [*not done yet*], plant immunity, pathogen behavior, and climate data to give a detailed picture of how the *Cercospora* disease spreads and affects coffee crops.

Our approach focuses on explaining the mechanisms of infection. We put a lot of emphasis on the spatial aspects of the pandemic, both within individual plants and across multiple plants in a

field. This helps us understand how the disease moves and develops under different environmental conditions.

Using climate data from the NASA POWER API, we ensured that our model reflects actual weather conditions, which is crucial for predicting outbreaks and planning effective interventions. The model helps identify the best conditions for disease development and the key factors that influence infection rates.

## Acknowledgement

We would like to express our gratitude to Véronique Letort Le Chevalier, who supervised this study and provided invaluable advice throughout the process. We extend our heartfelt thanks to Alain Zeitoun, our project teacher, for his invaluable feedback on improving the communication aspect during our presentations.

We also express our sincere appreciation to the CIRAD team for their active involvement and support. We are grateful to Houssem Triki, who supervised the project, created the MIMIC platform, and assisted us with the equations and models. Additionally, we thank Fabienne Ribeyre for her constructive feedback on the model and the article. Finally, we would like to express our sincere gratitude to Jacques Avelinot for generously sharing his expertise in the biology of infectious diseases, which proved to be incredibly valuable.

Their collective guidance and support have been instrumental in advancing this project.

## References

- Ali, Sajad, Anshika Tyagi, and Hanhong Bae. 2023. Plant microbiome: an ocean of possibilities for improving disease resistance in plants [in en]. *Microorganisms* 11, no. 2 (February).
- Bentham, Adam R, Juan Carlos De la Concepcion, Nitika Mukhi, Rafal Zdrzalek, Markus Draeger, Danylo Gorenkin, Richard K Hughes, and Mark J Banfield. 2020. A molecular roadmap to the plant immune system [in en]. *J. Biol. Chem.* 295, no. 44 (October): 14916–14935.
- Bock, KR. 1970. Plant pathology in east africa.
- Conrath, Uwe. 2006. Systemic acquired resistance [in en]. *Plant Signal. Behav.* 1, no. 4 (July): 179–184.
- Ding, Li-Na, Yue-Tao Li, Yuan-Zhen Wu, Teng Li, Rui Geng, Jun Cao, Wei Zhang, and Xiao-Li Tan. 2022. Plant disease resistance-related signaling pathways: recent progress and future prospects [in en]. *Int. J. Mol. Sci.* 23, no. 24 (December): 16200.
- Doughari, J, et al. 2015. An overview of plant immunity. *J. Plant Pathol. Microbiol* 6 (11): 10–4172.
- EU. 2020. *Robust project*. [https://capacity4dev.europa.eu/projects/desira/info/robust\\_en](https://capacity4dev.europa.eu/projects/desira/info/robust_en).
- F. van den Bosch, J. A. J. Metz, and J. C. Zadoks. 1999. Pandemics of focal plant disease, a model. *Phytopathology* 89:495–505. <https://doi.org/10.1094/PHYTO.1999.89.6.495>.
- Frédéric Boyer, Céline Gouwie. 2019. Gestion intégrée des maladies cercosporiose. *Institut Technique de la Bettrave*, [https://www.itbfr.org/fileadmin/user\\_upload/PDF/Fiches\\_Bioagresseurs/Gestion\\_integree\\_-\\_cercosporiose\\_web.pdf](https://www.itbfr.org/fileadmin/user_upload/PDF/Fiches_Bioagresseurs/Gestion_integree_-_cercosporiose_web.pdf).
- Imbusch, Frederike, Sebastian Liebe, Tobias Erven, and Mark Varrelmann. 2020. Dynamics of cercospora leaf spot disease determined by aerial spore dispersalin artificially inoculated sugar beet fields. *WILEY*.
- Kadhim Tayyeh, Halah, and Ruqayah Mohammed. 2023. Analysis of nasa power reanalysis products to predict temperature and precipitation in euphrates river basin. *Journal of Hydrology* 619:129327. issn: 0022-1694. <https://doi.org/https://doi.org/10.1016/j.jhydrol.2023.129327>. <https://www.sciencedirect.com/science/article/pii/S002216942300269X>.
- Kant, M R, W Jonckheere, B Knecht, F Lemos, J Liu, B C J Schimmel, C A Villarroel, et al. 2015. Mechanisms and ecological consequences of plant defence induction and suppression in herbivore communities [in en]. *Ann. Bot.* 115, no. 7 (June): 1015–1051.
- Muhammad, Tayeb, Fei Zhang, Yan Zhang, and Yan Liang. 2019. Rna interference: a natural immune system of plants to counteract biotic stressors [in en]. *Cells* 8, no. 1 (January): 38.
- NASA. 2024. *Nasa power*. <https://power.larc.nasa.gov/>.

- Ni, Hui-Fang, Ching-Yi Lin, and Chao-Jung Wu. 2020. Etiology and fungicide screening of coffee brown eye spot disease. *Journal of Taiwan Agricultural Research*, <https://scholars.tari.gov.tw/bitstream/123456789/15671/1/69-3-6.pdf>.
- Osborn, A E. 1996. Preformed antimicrobial compounds and plant defense against fungal attack [in en]. *Plant Cell* 8, no. 10 (October): 1821–1831.
- Prusinkiewicz, Przemyslaw, Mark Hammel, Jim Hanan, and Radomir Mech. 1996. L-systems: from the theory to visual models of plants. In *Proceedings of the 2nd csiro symposium on computational challenges in life sciences*, 3:1–32. Citeseer.
- RAM, M.RAGHU, and K. V. MALLAIAH. 1996. Effect of relative humidity on sporulation and germination of spores of cercospora and pseudocercospora spp. infecting legumes. *Indian Phytopath.*
- Rivillas, C. A. n.d. Berry blotch or iron spot. *Infectious Diseases. In Compendium*.
- Silva, Marília Goulart da, Edson Ampélio Pozza, Caio Vitor Rodrigues Vaz de Lima, and Tales Jesus Fernandes. 2015. Temperature and light intensity interaction on cercospora coffeicola sporulation and conidia germination.
- Sledz, Wojciech, Emilia Los, Agnieszka Paczek, Jacek Rischka, Agata Motyka, Sabina Zoledowska, Jacek Piosik, and Ewa Lojkowska. 2015. Antibacterial activity of caffeine against plant pathogenic bacteria [in en]. *Acta Biochim. Pol.* 62, no. 3 (August): 605–612.
- Triki, Houssein E. M., Fabienne Ribeyre, Fabrice Pinard, and Marc Jaeger. 2023. Coupling plant growth models and pest and disease models: an interaction structure proposal, mimic. *Plant Phenomics* 5:0077. <https://doi.org/10.34133/plantphenomics.0077>. eprint: <https://spj.science.org/doi/pdf/10.34133/plantphenomics.0077>. <https://spj.science.org/doi/abs/10.34133/plantphenomics.0077>.

## Appendix 1. Access to Code Repository

To facilitate the replication of our study and to promote transparency and reproducibility in research, we have made the code used for our modeling and analysis publicly available. The code can be accessed through our GitLab repository. The repository includes detailed instructions on how to set up the environment, run the models, and interpret the results.

**GitLab Repository:** <https://gitlab-student.centralesupelec.fr/mouad.leachouri/plant-pathogen-modelling>

### Appendix 1.1 Instructions for Accessing and Using the Code

#### 1. Clone the Repository:

```
git clone https://gitlab-student.centralesupelec.fr/
mouad.leachouri/plant-pathogen-modelling
```

- 2. Set Up the Environment:** Follow the instructions in the README.md file to set up the required environment and dependencies. This typically involves installing necessary packages and libraries. **Python 3.10** was used. If you want to make videos of the simulation you will need to install additionally ffmpeg.

```
pip install -r requirements.txt
```

- 3. Run the Models:** Detailed instructions on running the models are provided in the repository. For example, to run the main simulation script:

```
python main_simulation.py
```



## Appendix 2. Structure of the code

The code is run from the *main.py* file. It calls the *model* module, which contains our entire mathematical framework. Two additional folders exist in the main directory, *universe* and *video* which are output folders in which the model writes the results of the simulation and videos respectively.

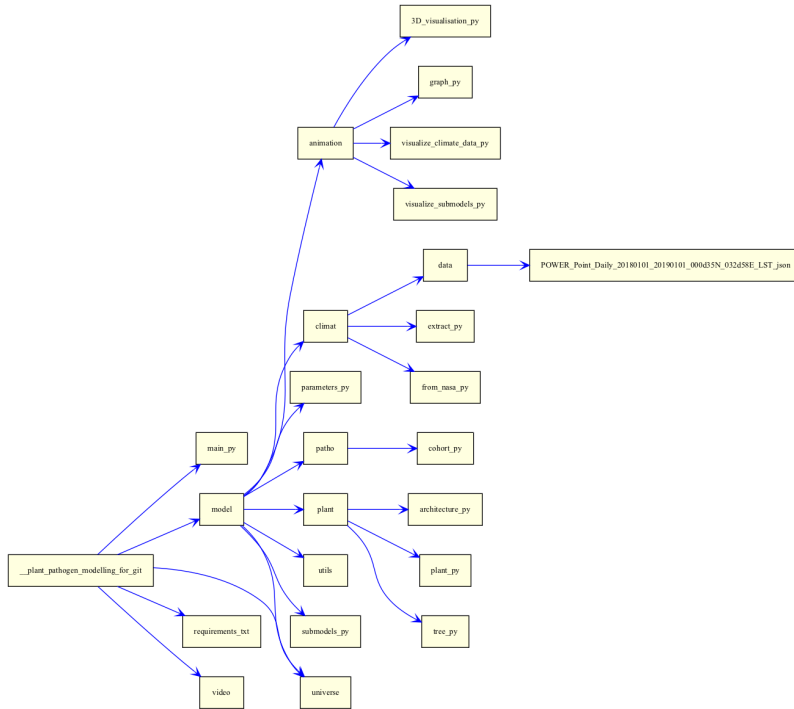


Figure 4. Project structure

We will now broadly go over the model to understand what it does. For clarity the *init.py* files have been removed.

- The *model* is composed of further submodules namely *patho*, *plant* which correspond to the pathogen and plant model respectively.
- The *utils* submodule provides the functions for the mathematical equations that the other submodels use.
- The *universe* submodule runs the simulation by bringing all other models into a class called *Universe*, which iteratively loops through time steps, updating the plant, pathogens, and climate data.
- The *model* also contains a *parameter.py* file with which you can tune the parameters of the simulation, such as the life cycle of the pathogen, the spore production rate, and video parameters.
- *climate* allows for the download and extraction of relevant climate data using NASA POWER API.
- *animation* provides functions for visualisation of the simulation results.

## Appendix 3. Contact Information

For any questions or further assistance, please contact the corresponding author at victor.rob-lam@student-cs.fr or mouad.leachouri@student-cs.fr.